This article is made available via the ACS COVID-19 subset for unrestricted RESEARCH re-use and analyses in any form or by any means with acknowledgement of the original source. These permissions are granted for the duration of the World Health Organization (WHO) declaration of COVID-19 as a global pandemic.

ACS APPLIED BIO MATERIALS

www.acsabm.org

Article

Codelivery of SARS-CoV-2 Prefusion-Spike Protein with CBLB502 by a Dual-Chambered Ferritin Nanocarrier Potentiates Systemic and Mucosal Immunity

Shubing Tang,*,⊥ Min Li,⊥ Lixiang Chen,⊥ Aguang Dai, Zhi Liu, Mangteng Wu, Jingyi Yang, Hongyun Hao, Jingdan Liang, Xiaohui Zhou,* and Zhikang Qian*

Cite This: https://doi.org/10.1021/acsabm.2c00328

Read Online

ACCESS | Metrics & More | Article Recommendations | Supporting Information

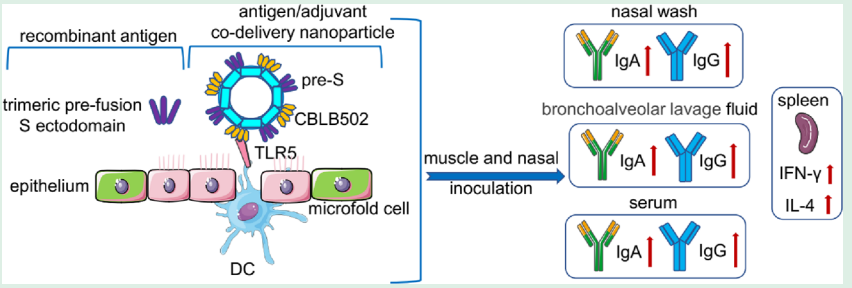

ABSTRACT: Thousands of breakthrough infections are confirmed after intramuscular (i.m.) injection of the approved vaccines against severe acute respiratory syndrome coronavirus 2 (SARS-CoV-2). Two major factors might contribute to breakthrough infections. One is the emergence of mutant variants of SARS-CoV-2, and the other is that i.m. injection has an inefficient ability to activate mucosal immunity in the upper respiratory tract. Here, we devised a dual-chambered nanocarrier that can codeliver the adjuvant CBLB502 with prefusion-spike (pre-S) onto a ferritin nanoparticle. This vaccine enabled enhanced systemic and local mucosal immunity in the upper and lower respiratory tract. Further, codelivery of CBLB502 with pre-S induced a Th1/Th2-balanced immunoglobulin G response. Moreover, the codelivery nanoparticle showed a Th1-biased cellular immune response as the release of splenic INF-γ was significantly heightened while the level of IL-4 was elevated to a moderate extent. In general, the developed dual-chambered nanoparticle can trigger multifaceted immune responses and shows great potential for mucosal vaccine development.

KEYWORDS: *codelivery, prefusion-spike, CBLB502, dual-chambered, ferritin nanocarrier, systemic and mucosal immunity*

INTRODUCTION

The pandemic of coronavirus disease 2019 caused by SARS-CoV-2 led to over 481 million recorded cases and over 6 million deaths worldwide until March 30, 2022 (https://covid19.who.int/). Hundreds of preclinical and clinical trials have been conducted to avert SARS-CoV-2 global transmission, and the principal target is spike (S) protein.[1] S protein distributes on a virion surface and forms a homotrimer protrusion, which interacts with its major receptor angiotensin-converting enzyme 2 (ACE2) and mediates virus entry.[2,3] S protein is cleaved into S1 and S2 at furin sites (residues 682−685) and undergoes conformational changes from prefusion to postfusion during the viral entry process.[4,5] The introduction of a "GSAS" substitution at furin sites and proline substitutions at residues 986 and 987 (S-2P) confer S protein in the prefusion conformation,[6,7] and this prefusion-spike (pre-S) is adopted as a promising vaccine candidate.[8,9]

Several vaccines have received emergency-use authorization (EUA) and induce robust humoral and cellular immunity by intramuscular (i.m.) injection.[10] Although systemic vaccination is effective for curtailing severe disease and mortality, it fails to elicit substantial mucosal (immunoglobulin A [IgA]) immunity and only provides suboptimal protection in the nasal turbinate (NT).[11,12] The nose is one of the primary entry routes for SARS-CoV-2 and acts as its initial reservoir.[13] Thus, generation of nasal IgA is vital for prevention of nasal SARS-CoV-2 acquisition and transmission. Intranasal (i.n.) vaccination of subunit vaccines against SARS-CoV-2 with adenovirus-vectored vaccines[14,15] or influenza-based vaccines[16] has induced substantive mucosal, systemic, and cellular immunity and supplied optimal protection against upper and lower respiratory tract (URT and LRT)

Received: April 7, 2022
Accepted: June 13, 2022

© XXXX American Chemical Society

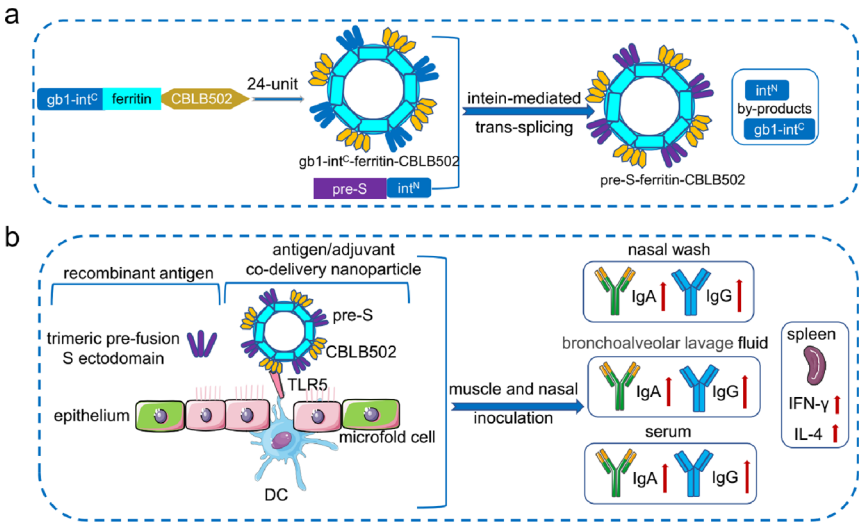

Figure 1. Schematic depiction of the rationale of the dual-chambered ferritin nanocarrier and its adjuvant effects. (a) The 24-unit gb1-int^C-ferritin-CBLB502 proteins spontaneously assemble the dual-chambered nanocarrier. The desired cargo, pre-S, is covalently coupled onto the nanoparticle surface to generate the codelivery nanoparticle pre-S-ferritin-CBLB502. (b) The codelivery nanoparticle targets DCs in the nasal area through the interaction of the TLR5 agonist with TLR5 and induces increased IgA and IgG responses in the nasal wash (NW), bronchoalveolar lavage fluid (BALF), and serum. In addition, the production of IFN-γ and IL-4 by splenocytes will also be upregulated.

infection.[17] However, other effective novel vaccines are still needed with regard to safety and compatibility.

Soluble antigens are safe vaccine candidates but possess two drawbacks for intranasal vaccination. One is that they are less immunogenic than the authentic virus,[10] and the second is that they are inefficiently transported across the epithelial barrier by microfold (M) cells to be presented to dendritic cells (DCs).[18] Nanoparticles have been designed to penetrate the mucosal barrier for antigen delivery or for therapeutic application.[19,20] In addition, nanoparticle combinations with adjuvants have been utilized to improve protein immunogenicity.[21] The 24-unit *Helicobacter pylori* (*H. pylori*) ferritin spontaneously assembles nanoparticles harboring eight three-fold symmetric axes,[22] which has shown excellent potential in enhancing immune responses for trimeric antigens like influenza hemagglutinin[23] or EBV glycoprotein 350.[24] Ectodomains of S protein have been displayed onto *H. pylori* ferritin and have been formulated with different adjuvants to facilitate immune responses.[25−27] Flagellin is an agonist of Toll-like receptor (TLR) 5 and serves as a potent adjuvant in enhancing parenteral and mucosal vaccination.[28,29] However, flagellin or its derivative, CBLB502, tends to aggregate, and thus, denaturing and refolding processes are needed when flagellin is genetically linked to an antigen.[30,31] In other words, it remains a great challenge to codeliver a mucosal adjuvant with an antigen onto a single nanoparticle.

In recent years, modular nanoparticle display technology has been attracting more and more attention to load various payloads. Proteins can be covalently coupled to nanoparticles by sortase,[32,33] while transpeptidation mediated by this enzyme is a reversible reaction and precludes its application potential. SpyCatcher/SpyTag is an intriguing covalent peptide tagging technology and has been utilized to display SARS-CoV-2 antigens.[34−36] As the retained SpyCatcher/SpyTag might raise unwarranted nonspecific immune responses, we have developed intein-mediated trans-splicing, which cleaves itself during the coupling process to load protein-based cargos onto nanoparticles.[37−39] Previous studies and our work mainly focus on coupling cargos to a single insertion site on a nanoparticle surface. When an antigen and an adjuvant are codelivered, it is difficult to generate homogeneous products across multiple batches.[40] Inspired by the concept of a double-chambered ferritin platform,[41] we aim to expand the delivery capability of a ferritin nanocarrier by combinational use of intein-mediated trans-splicing with genetic fusion. We introduced a split intein^C moiety to the ferritin N-terminus to load pre-S by intein-mediated trans-splicing, while we genetically fused CBLB502 to the ferritin C-terminus. Interestingly, we found that this codelivery nanoparticle offered comprehensive adjuvant effects, including elevating spike-specific systemic immunity, heightening local mucosal immunity in the upper and lower respiratory tract, and augmenting cellular immunity in the spleen.

MATERIALS AND METHODS

To generate a dual-chambered ferritin nanocarrier, gb1-intein^C was placed to the ferritin N-terminus,[37] and CBLB502 was genetically fused to the ferritin C-terminus (Figure S1).[41] A recombinant gene was cloned to the pET28a vector and was expressed by BL21 (DE3) plysS. An ectodomain of pre-S (1−1208) with a foldon tag at its C-terminus[6] was fused to split intein^N,[37] and protein pre-S-int^N was expressed by an ExpiCHO expression system. Genetic fusion of the ectodomain of pre-S (1−1208) to *H. pylori* ferritin worked as a control nanoparticle that was expressed by Expi293F cells. A recombinant plasmid, pCDNA3.1+ pre-S-ferritin, was transfected into Expi293F cells by EZ Trans-II (Shanghai Life iLab Biotech Co., Ltd.). Incubation of the dual-chambered ferritin nanocarrier, gb1-int^C-ferritin-CBLB502, with pre-S-int^N would generate a codelivery pre-S-ferritin-CBLB502 nanoparticle that was recovered from the reaction mixture by a ClearFirst-3000 protein purification system of Shanghai Flash Spectrum Biological Technology Co., Ltd. Detailed information is supplied on the Supporting Information.

RESULTS AND DISCUSSION

The Rationale of the Dual-Chambered Ferritin Nanocarrier. We have developed ferritin as a modular nanocarrier by intein-mediated trans-splicing, which resulted in equipment of desired cargos onto its N-terminus.[38] Although an antigen and an adjuvant can be concurrently conjugated to a ferritin nanoparticle, it is difficult to precisely constrain their mole ratio. Furthermore, having only one insertion site is another

https://doi.org/10.1021/acsabm.2c00328
ACS Appl. Bio Mater. XXXX, XXX, XXX−XXX

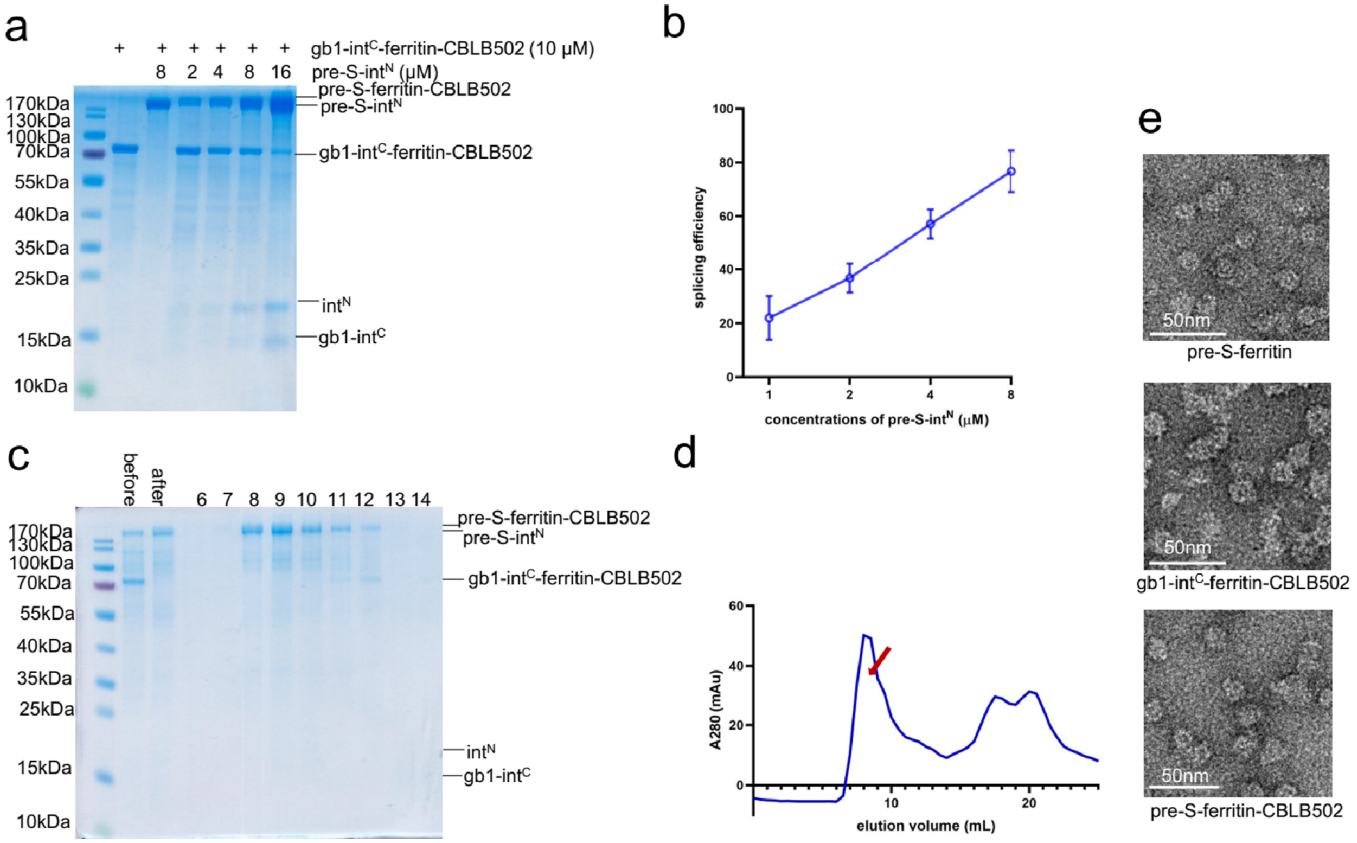

Figure 2. Optimization of in vitro trans-splicing, generation, and characterization of the codelivery nanoparticle. (a) Two-fold increase in the pre-S-int^N concentration to achieve high reaction efficiency. (b) Semiquantification of trans-splicing efficiency by ImageJ and GraphPad Prism 8.0. The plot represented values of three repeats with the standard error of the mean (±SEM). (c) Coomassie brilliant blue (CBB) staining analysis of the recovery of the codelivery nanoparticle by gel filtration. (d) UV profile of the recovery of the codelivery nanoparticle by gel filtration. (e) TEM images of pre-S-ferritin, gb1-int^C-ferritin-CBLB502, and pre-S-ferritin-CBLB502.

limiting factor. A previous study has proposed proof of concept of double-chambered nanocages[41] that sheds light on the possibility to expand the loading capability of the ferritin nanocarrier. To this end, we devise a dual-chambered ferritin nanocarrier. We insert gb1-int^C to the N-terminus of ferritin and fuse CBLB502 to its C-terminus to make gb1-int^C-ferritin-CBLB502, which reacts with pre-S-int^N to generate an antigen/adjuvant codelivery nanoparticle, pre-S-ferritin-CBLB502 (Figure 1a and Figure S1a,b).

A codelivery nanoparticle benefits not only from the inherent properties of the nanoparticle but also from the adjuvant effects activated by CBLB502. Nanoscale particles are favorably internalized by antigen-presenting cells (APCs); the multivalent display of an antigen in a repetitive manner facilitates B cell activation, memory B cell proliferation, and so on.[42] The TLR5 agonist interacts with the TLR5 on the surface of M cells and DCs and stimulates robust mucosal and systemic immune responses.[43,44] We envision that this codelivery nanoparticle will improve IgA and IgG responses in the URT and the LRT while promoting systemic immunity. In addition, this codelivery nanoparticle will strength cellular responses (Figure 1b).

Generation and Characterization of the Codelivery Nanoparticle. First, we investigated the feasibility of codelivering pre-S with CBLB502 onto a ferritin nanoparticle. A recombinant clone, gb1-int^C-ferritin-CBLB502, was constructed, and the dual-chambered ferritin nanocarrier was manufactured by a denaturation and renaturation process (Figure S1a,c). The cargo protein, pre-S-int^N-6xHis (pre-S-int^N for short), was purified by Ni^{2+} resin. The nanoparticle fused with pre-S, pre-S-ferritin, was purified by ultracentrifugation (Figure S1a,d). We performed dose-dependent assay and found that a sufficient concentration of pre-S-int^N led to a high yield of >80% (Figure 2a,b). We applied the mixture to a Superose 6 increase column to attain the target product after the reaction (Figure 2c,d). We imaged samples of pre-S-ferritin, gb1-int^C-ferritin-CBLB502, and pre-S-ferritin-CBLB502 by transmission electron microscopy (TEM) and observed that the aforementioned proteins retained their nanoscale spherical morphology (Figure 2e). Taken together, our data confirmed that it was amenable to codeliver pre-S with CBLB502 onto a ferritin nanoparticle.

Assessment of Systemic Immunity. We next evaluated the adjuvant effects in a C57BL/6J-TgN (hACE2) mouse model. Previous clinical data indicated that solely intranasal vaccination against SARS-CoV-2 was inefficient to confer substantial immunity,[45] while heterologous prime-boost immunizations conferred robust immunity.[16,46] To this end, mice received two i.m. injections and one i.n. immunization with different regimens (Figure 3a). Mice were divided into five groups: ferritin, pre-S, pre-S-ferritin, an admixture of pre-S-ferritin with CBLB502 (pre-S-ferritin+CBLB502), and the codelivery nanoparticle (pre-S-ferritin-CBLB502). After three inoculations, spike-specific antibody responses were analyzed in NW, BALF, and serum, whereas cellular responses were inspected in the spleens.

https://doi.org/10.1021/acsabm.2c00328
ACS Appl. Bio Mater. XXXX, XXX, XXX−XXX

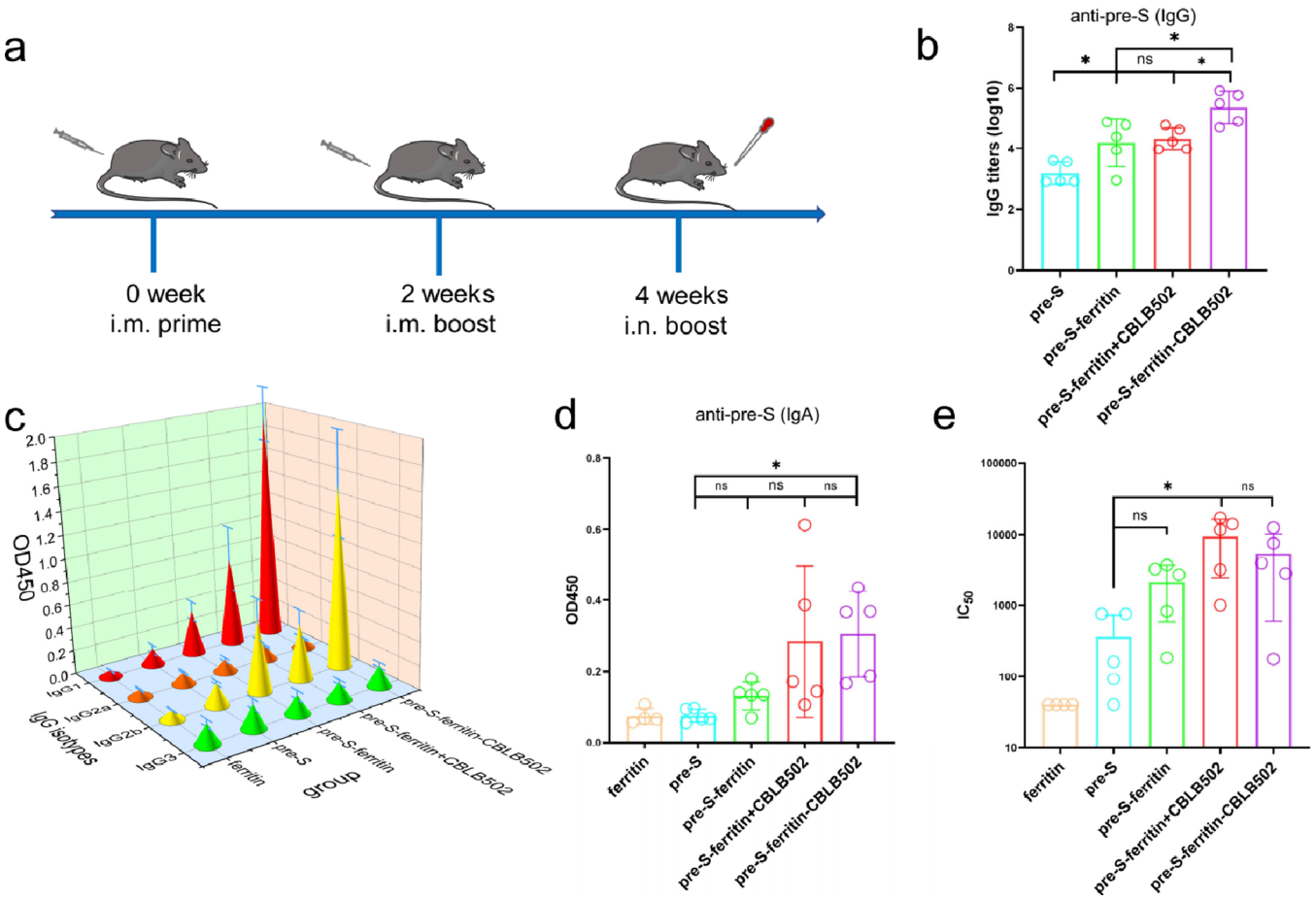

Figure 3. Evaluation of systemic antibody response. Sera were collected two weeks after the third inoculation, and samples were used for ELISA and neutralizing assays. (a) Immunization schedule for C57BL/6J-TgN (hACE2). (b) Spike-specific IgG titers were determined by enzyme-linked immunosorbent assay (ELISA). (c) IgG isotype assay. (d) IgA responses in serum. (e) IC_{50} of neutralizing antibodies. Statistical significance was denoted by the following symbols: ns = not significant and $*p < 0.05$.

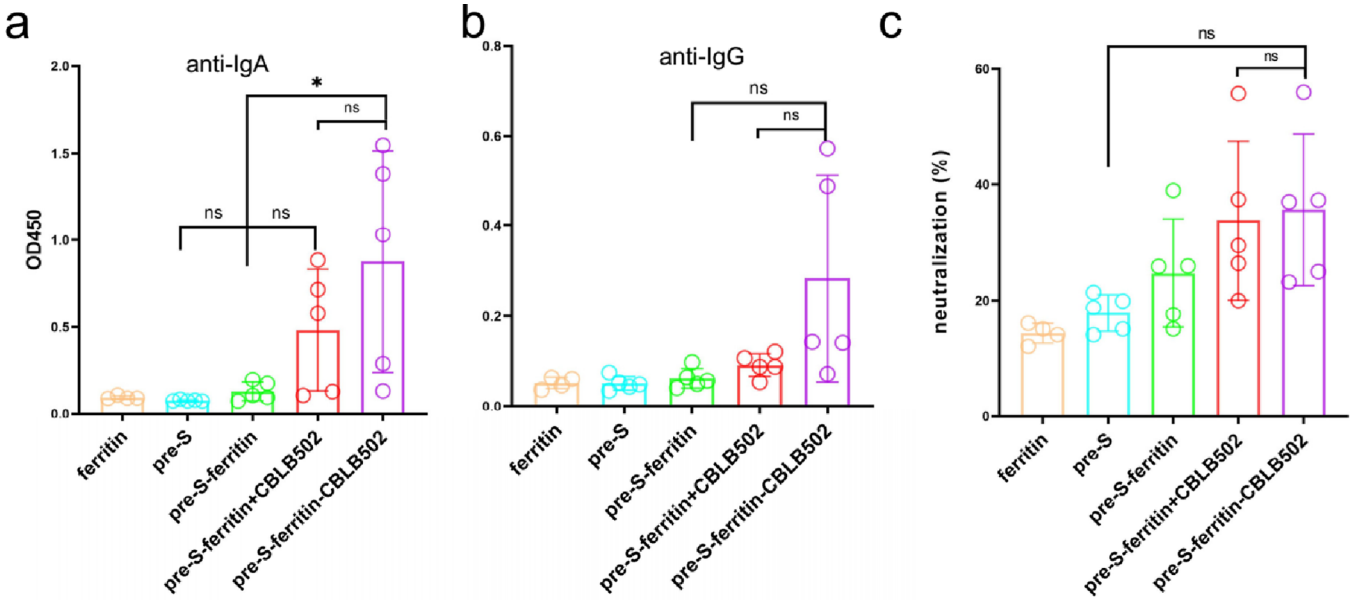

Figure 4. Local mucosal antibody responses in the URT. Three weeks after the third injection, nasal wash samples were collected for immunization assays. Spike-specific IgA (a) and IgG (b) responses were detected by ELISA, and NW samples were diluted to 1:5 and 1:10, respectively. (c) Neutralizing efficiency of samples measured with a dilution of 1:8. Statistical significance was presented as follows: ns = not significant and $*p < 0.05$.

https://doi.org/10.1021/acsabm.2c00328
ACS Appl. Bio Mater. XXXX, XXX, XXX−XXX

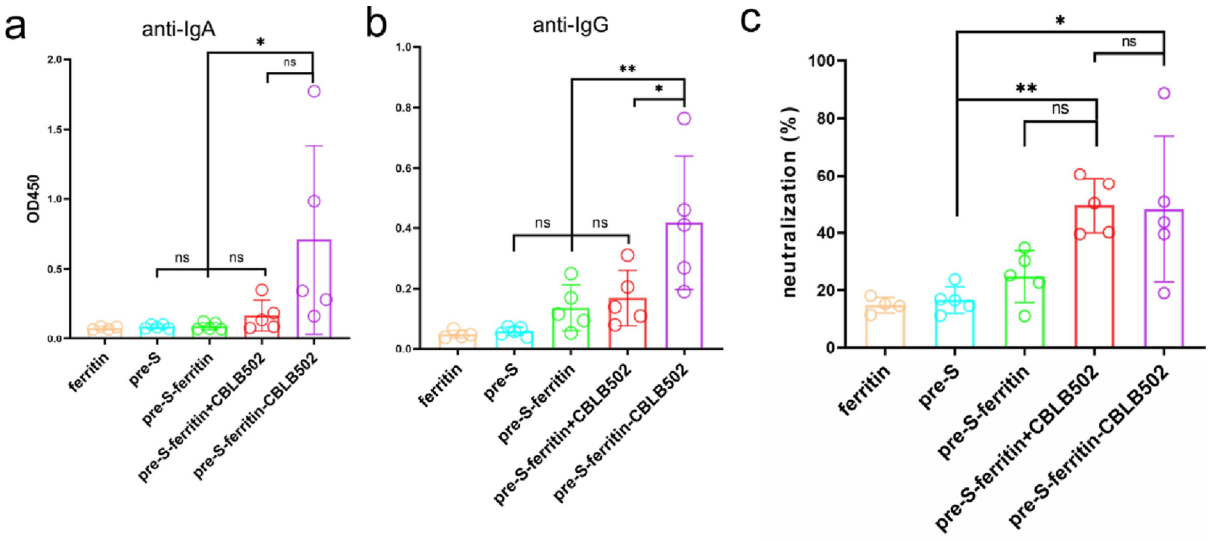

Figure 5. Local mucosal antibody responses in the LRT. BALF samples were obtained three weeks after the third injection for immunization assays. Spike-specific IgA (a) and IgG (b) responses were measured by ELISA, and BALF samples were diluted to 1:5 and 1:10, respectively. (c) BALF samples were diluted to 1:8 to determine the pseudovirus neutralizing efficiency. Statistical significance was depicted by the following symbols: ns = not significant, $*p < 0.05$, and $**p < 0.01$.

In serum samples, four groups comprising the pre-S antigen yielded high titers of spike-specific IgG (Figure 3b). The codelivery nanoparticle elicited the strongest antispike IgG responses (mean, 4.87; log range, 4.1−6.2), whereas pre-S-ferritin+CBLB502 sustained slightly improved IgG responses compared to pre-S-ferritin (mean logs: 4.24 vs 4.2). Moreover, statistical significance assay revealed that pre-S-ferritin-CBLB502 triggered notably higher IgG responses compared with pre-S-ferritin+CBLB502 (Figure 3b). To gain further insight into the profile of antibody responses, IgG isotype assays were conducted with a dilution of 1:10.[4] Strikingly, the codelivery nanoparticle augmented both IgG1 and IgG2b responses (Figure 3c). To further explore the adjuvant effect raised by the codelivery nanoparticle, we measured spike-specific IgG1 and IgG2b titers. We found that pre-S-ferritin-CBLB502 moderately enhanced IgG1 responses compared to pre-S-ferritin+CBLB502 (Figure S2a), while it exhibited excellent adjuvant properties on improving IgG2b responses (Figure S2b). To consider that pre-S-ferritin-CBLB502 induced comparable IgG1 and IgG2b responses (Figure 3c), we envisioned that it conferred Th1/Th2-balanced responses. In addition, the codelivery nanoparticle provoked remarkably increased IgA responses compared to pre-S (mean OD450: 0.30 vs 0.06) (Figure 3d). The 50% inhibitory concentrations (IC_{50}) of each group were determined (Figure S2c−g), and the trends of the neutralizing antibody were consistent with IgG titers (Figure 3e). In general, the codelivery nanoparticle conferred pronouncedly improved humoral responses.

Local Mucosal Immunity in the URT. Secretion of IgA can neutralize and block virus entry in the URT where SARS-CoV-2 entry occurs and is critical for completely sterilizing SARS-CoV-2 infection.[16,46] Thus, we collected nasal wash (NW) samples and explored the antibody responses in the URT. We observed that the codelivery nanoparticle launched significantly stronger IgA responses than those of pre-S-ferritin (Figure 4a). Furthermore, the codelivery nanoparticle also mounted IgG responses, albeit to a moderate extent (Figure 4b). Finally, the virus-neutralizing capability was improved in a nonsignificant magnitude by the codelivery nanoparticle (Figure 4c). In a word, local mucosal immunity in the URT was heighted by the codelivery nanoparticle.

Local Mucosal Immunity in the LRT. We next harvested BALF samples and detected antibody responses in the LRT. We found that the codelivery nanoparticle induced significant higher levels of antigen-specific IgA (Figure 5a) and IgG (Figure 5b) than those of pre-S-ferritin, whereas the admixture of pre-S-ferritin with CBLB502 (pre-S-ferritin+CBLB502) showed a moderate enhancement effect (Figure 5a,b). In addition, it is worth noting that pre-S-ferriin-CBLB502 induced substantially higher IgG responses than those of pre-S-ferritin+CBLB502 (Figure 5b). Moreover, the codelivery nanoparticle provoked a notably improved neutralizing capability compared to pre-S in the BALF samples (Figure 5c). In general, the codelivery nanoparticle elevated local mucosal immunity in the LRT.

Cellular Immunity in the Spleen. Cellular responses are very important to design an effective vaccine against SARS-CoV-2.[47] To identify the type of cellular immunity, splenocytes were harvested three weeks after the third immunization and were in vitro restimulated by pre-S-int^N protein. Enzyme-linked immunospot assay (ELISPOT) was performed to determine the levels of IFN-γ and IL-4. Compared with other vaccine regimens, pre-S-ferritin-CBLB502 provoked the highest level of IFN-γ and IL-4 (Figure 6a−c). Strikingly, we observed that pre-S-ferritin-CBLB502 significantly improved IFN-γ responses compared to pre-S-ferritin+CBLB502 (Figure 6a). Although pre-S-ferritin-CBLB502 enabled facilitating IL-4 responses compared to pre-S-ferritin+CBLB502, the enhancement effect was moderate (Figure 6b). Moreover, pre-S-ferritin-CBLB502 elicited much stronger IFN-γ responses than those of IL-4 as the mean number of positive spots per 5×10^5 cells of IFN-γ was much higher than that of IL-4 (mean: 167.8 vs 45.8). As Th1 cells produce IFN-γ and Th2 secretes IL-4,[48] our results suggested that pre-S-ferritin-CBLB502 profoundly enhanced cellular immunity in a Th1-biased manner.

CONCLUSIONS

Nanoparticles together with adjuvants are widely and increasingly used to improve the immunogenicity of subunit vaccines.

https://doi.org/10.1021/acsabm.2c00328
ACS Appl. Bio Mater. XXXX, XXX, XXX−XXX

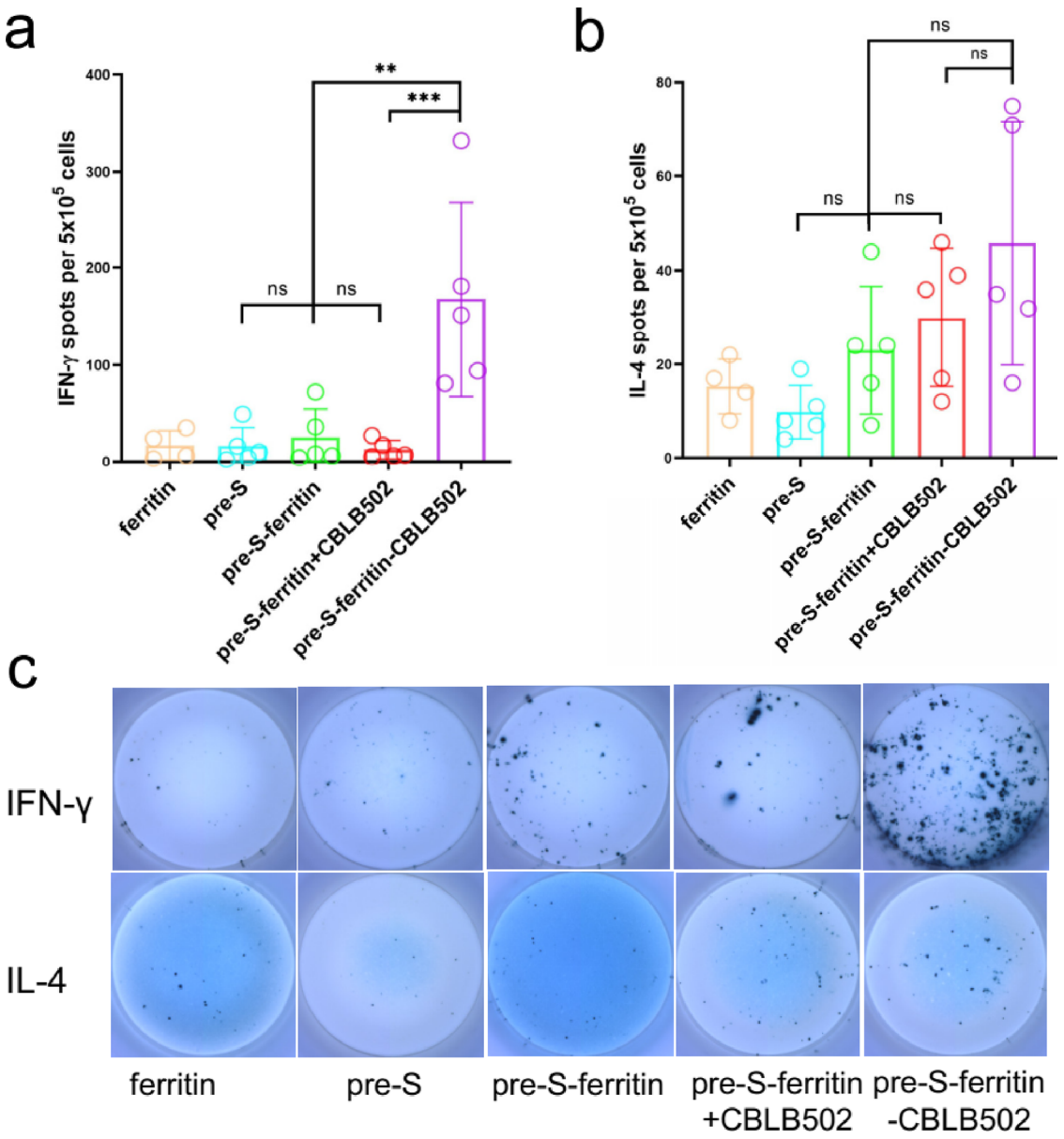

Figure 6. Cellular immunity in the spleen. (a) Detection of IFN-γ levels by ELISPOT. (b) Determination of IL-4 levels. (c) Representative images of ELISPOT assays for IFN-γ (upper panel) and IL-4 (lower panel). Statistical significance was denoted by the following symbols: ns = not significant, *$p < 0.05$, **$p < 0.01$, and ***$p < 0.001$.

However, adjuvant proteins tend to aggregate or form inclusion bodies,[28,29,37] and researchers encounter a great challenge to codeliver an antigen with an adjuvant. To this end, we developed a dual-chambered ferritin nanocarrier, gb1-int^C-ferritin-CBLB502, which was expressed by *Escherichia coli* with a yield of over 50 mg/L. An antigen, pre-S-int^N, was expressed by eukaryotes and was covalently conjugated to the engineered ferritin nanocarrier in a facile and efficient fashion. Since then, the denaturation and renaturation processes caused by adjuvant proteins, which have detrimental effects on the authentic properties of antigens, can be avoided. An in vivo immunization study demonstrated that the codelivery nanoparticle, pre-S-ferritin-CBLB502, substantially improved systemic immunity, local mucosal immunity in the URT and LRT, and cellular immunity. As intein-mediated trans-splicing is a modular technology, we speculate that the proposed dual-chambered ferritin nanocarrier can be used to load other antigens and bring benefits for mucosal vaccine development.

■ ASSOCIATED CONTENT

Supporting Information

The Supporting Information is available free of charge at https://pubs.acs.org/doi/10.1021/acsabm.2c00328.

Materials and methods; constructs of clones; engineered nanoparticle gb1-int^C-ferritin-CBLB502 purification and genetic fusion of pre-S-ferritin nanoparticle purification; IgG1 and IgG2b titers and neutralizing titers of mouse sera (PDF)

■ AUTHOR INFORMATION

Corresponding Authors

Shubing Tang − *Shanghai Public Health Clinical Center, Fudan University, 201058 Shanghai, China;* Present

https://doi.org/10.1021/acsabm.2c00328
ACS Appl. Bio Mater. XXXX, XXX, XXX−XXX

Address: Ruizhou Biotech Co., Ltd., 201210 Shanghai, China (S.T.); orcid.org/0000-0001-6639-0222; Email: tangshubing@163.com

Xiaohui Zhou − *Shanghai Public Health Clinical Center, Fudan University, 201058 Shanghai, China*; Email: zhouxiaohui@shphc.org.cn

Zhikang Qian − *Shanghai Public Health Clinical Center, Fudan University, 201058 Shanghai, China*; Email: zkqian72@126.com

Authors

Min Li − *Shanghai Public Health Clinical Center, Fudan University, 201058 Shanghai, China*

Lixiang Chen − *Shanghai Public Health Clinical Center, Fudan University, 201058 Shanghai, China*

Aguang Dai − *CAS Key Laboratory of Molecular Virology & Immunology, Institut Pasteur of Shanghai, Chinese Academy of Sciences, University of the Chinese Academy of Sciences, 200031 Shanghai, China*

Zhi Liu − *CAS Key Laboratory of Molecular Virology & Immunology, Institut Pasteur of Shanghai, Chinese Academy of Sciences, University of the Chinese Academy of Sciences, 200031 Shanghai, China*

Mangteng Wu − *CAS Key Laboratory of Molecular Virology & Immunology, Institut Pasteur of Shanghai, Chinese Academy of Sciences, University of the Chinese Academy of Sciences, 200031 Shanghai, China*

Jingyi Yang − *Shanghai Public Health Clinical Center, Fudan University, 201058 Shanghai, China*

Hongyun Hao − *Shanghai Public Health Clinical Center, Fudan University, 201058 Shanghai, China*

Jingdan Liang − *State Key Laboratory of Microbial Metabolism, College of Life Sciences and Biotechnology, Shanghai Jiao Tong University, 200030 Shanghai, China*

Complete contact information is available at: https://pubs.acs.org/10.1021/acsabm.2c00328

Author Contributions

[⊥]S.T., M.L., and L.C. conducted major experiments and contributed equally to this manuscript. Z.Q., X.Z., and S.T. conceived and designed the experiments. Z.L. and A.D. collected TEM data. M.W., J.Y., and H.H. provided help in different experiments. S.T. wrote and J.L. revised the manuscript. All authors have given approval to the final version of the manuscript.

Funding

This manuscript is founded by the General Program of the National Natural Science Foundation of China (grant number 32070928) and partially supported by the Open Funding Project of the State Key Laboratory of Microbial Metabolism (grant number MMLKF19-09).

Notes

The authors declare no competing financial interest.

■ ACKNOWLEDGMENTS

Negative staining TEM data were collected at the core facility of Biological Imaging, Institut Pasteur of Shanghai (IPS), CAS. The SARS-CoV-2 pseudovirus is a gift from Professor Jianqing Xu, Fudan University.

■ REFERENCES

(1) Dai, L.; Gao, G. F. Viral targets for vaccines against COVID-19. *Nat. Rev. Immunol.* **2021**, *21*, 73−82.

(2) Yao, H.; Song, Y.; Chen, Y.; Wu, N.; Xu, J.; Sun, C.; Zhang, J.; Weng, T.; Zhang, Z.; Wu, Z.; Cheng, L.; Shi, D.; Lu, X.; Lei, J.; Crispin, M.; Shi, Y.; Li, L.; Li, S. Molecular Architecture of the SARS-CoV-2 Virus. *Cell* **2020**, *183*, 730−738.e13.

(3) Ke, Z.; Oton, J.; Qu, K.; Cortese, M.; Zila, V.; McKeane, L.; Nakane, T.; Zivanov, J.; Neufeldt, C. J.; Cerikan, B.; Lu, J. M.; Peukes, J.; Xiong, X.; Krausslich, H. G.; Scheres, S. H. W.; Bartenschlager, R.; Briggs, J. A. G. Structures and distributions of SARS-CoV-2 spike proteins on intact virions. *Nature* **2020**, *588*, 498−502.

(4) Hoffmann, M.; Kleine-Weber, H.; Schroeder, S.; Kruger, N.; Herrler, T.; Erichsen, S.; Schiergens, T. S.; Herrler, G.; Wu, N. H.; Nitsche, A.; Muller, M. A.; Drosten, C.; Pohlmann, S. SARS-CoV-2 Cell Entry Depends on ACE2 and TMPRSS2 and Is Blocked by a Clinically Proven Protease Inhibitor. *Cell* **2020**, *181*, 271−280.e8.

(5) Walls, A. C.; Park, Y. J.; Tortorici, M. A.; Wall, A.; McGuire, A. T.; Veesler, D. Structure, Function, and Antigenicity of the SARS-CoV-2 Spike Glycoprotein. *Cell* **2020**, *181*, 281−292.e6.

(6) Wrapp, D.; Wang, N.; Corbett, K. S.; Goldsmith, J. A.; Hsieh, C. L.; Abiona, O.; Graham, B. S.; McLellan, J. S. Cryo-EM structure of the 2019-nCoV spike in the prefusion conformation. *Science* **2020**, *367*, 1260−1263.

(7) Hsieh, C. L.; Goldsmith, J. A.; Schaub, J. M.; DiVenere, A. M.; Kuo, H. C.; Javanmardi, K.; Le, K. C.; Wrapp, D.; Lee, A. G.; Liu, Y.; Chou, C. W.; Byrne, P. O.; Hjorth, C. K.; Johnson, N. V.; Ludes-Meyers, J.; Nguyen, A. W.; Park, J.; Wang, N.; Amengor, D.; Lavinder, J. J.; Ippolito, G. C.; Maynard, J. A.; Finkelstein, I. J.; McLellan, J. S. Structure-based design of prefusion-stabilized SARS-CoV-2 spikes. *Science* **2020**, *369*, 1501−1505.

(8) Corbett, K. S.; Edwards, D. K.; Leist, S. R.; Abiona, O. M.; Boyoglu-Barnum, S.; Gillespie, R. A.; Himansu, S.; Schafer, A.; Ziwawo, C. T.; DiPiazza, A. T.; Dinnon, K. H.; Elbashir, S. M.; Shaw, C. A.; Woods, A.; Fritch, E. J.; Martinez, D. R.; Bock, K. W.; Minai, M.; Nagata, B. M.; Hutchinson, G. B.; Wu, K.; Henry, C.; Bahl, K.; Garcia-Dominguez, D.; Ma, L.; Renzi, I.; Kong, W. P.; Schmidt, S. D.; Wang, L.; Zhang, Y.; Phung, E.; Chang, L. A.; Loomis, R. J.; Altaras, N. E.; Narayanan, E.; Metkar, M.; Presnyak, V.; Liu, C.; Louder, M. K.; Shi, W.; Leung, K.; Yang, E. S.; West, A.; Gully, K. L.; Stevens, L. J.; Wang, N.; Wrapp, D.; Doria-Rose, N. A.; Stewart-Jones, G.; Bennett, H.; Alvarado, G. S.; Nason, M. C.; Ruckwardt, T. J.; McLellan, J. S.; Denison, M. R.; Chappell, J. D.; Moore, I. N.; Morabito, K. M.; Mascola, J. R.; Baric, R. S.; Carfi, A.; Graham, B. S. SARS-CoV-2 mRNA vaccine design enabled by prototype pathogen preparedness. *Nature* **2020**, *586*, 567−571.

(9) Mercado, N. B.; Zahn, R.; Wegmann, F.; Loos, C.; Chandrashekar, A.; Yu, J.; Liu, J.; Peter, L.; McMahan, K.; Tostanoski, L. H.; He, X.; Martinez, D. R.; Rutten, L.; Bos, R.; van Manen, D.; Vellinga, J.; Custers, J.; Langedijk, J. P.; Kwaks, T.; Bakkers, M. J. G.; Zuijdgeest, D.; Rosendahl Huber, S. K.; Atyeo, C.; Fischinger, S.; Burke, J. S.; Feldman, J.; Hauser, B. M.; Caradonna, T. M.; Bondzie, E. A.; Dagotto, G.; Gebre, M. S.; Hoffman, E.; Jacob-Dolan, C.; Kirilova, M.; Li, Z.; Lin, Z.; Mahrokhian, S. H.; Maxfield, L. F.; Nampanya, F.; Nityanandam, R.; Nkolola, J. P.; Patel, S.; Ventura, J. D.; Verrington, K.; Wan, H.; Pessaint, L.; Van Ry, A.; Blade, K.; Strasbaugh, A.; Cabus, M.; Brown, R.; Cook, A.; Zouantchangadou, S.; Teow, E.; Andersen, H.; Lewis, M. G.; Cai, Y.; Chen, B.; Schmidt, A. G.; Reeves, R. K.; Baric, R. S.; Lauffenburger, D. A.; Alter, G.; Stoffels, P.; Mammen, M.; Van Hoof, J.; Schuitemaker, H.; Barouch, D. H. Single-shot Ad26 vaccine protects against SARS-CoV-2 in rhesus macaques. *Nature* **2020**, *586*, 583−588.

(10) Jeyanathan, M.; Afkhami, S.; Smaill, F.; Miller, M. S.; Lichty, B. D.; Xing, Z. Immunological considerations for COVID-19 vaccine strategies. *Nat. Rev. Immunol.* **2020**, *20*, 615−632.

(11) Zhou, D.; Chan, J. F.; Zhou, B.; Zhou, R.; Li, S.; Shan, S.; Liu, L.; Zhang, A. J.; Chen, S. J.; Chan, C. C.; Xu, H.; Poon, V. K.; Yuan, S.; Li, C.; Chik, K. K.; Chan, C. C.; Cao, J.; Chan, C. Y.; Kwan, K. Y.; Du, Z.; Lau, T. T.; Zhang, Q.; Zhou, J.; To, K. K.; Zhang, L.; Ho, D. D.; Yuen, K. Y.; Chen, Z. Robust SARS-CoV-2 infection in nasal turbinates after

treatment with systemic neutralizing antibodies. *Cell Host Microbe* **2021**, *29*, 551−563.e5.
(12) Vogel, A. B.; Kanevsky, I.; Che, Y.; Swanson, K. A.; Muik, A.; Vormehr, M.; Kranz, L. M.; Walzer, K. C.; Hein, S.; Guler, A.; Loschko, J.; Maddur, M. S.; Ota-Setlik, A.; Tompkins, K.; Cole, J.; Lui, B. G.; Ziegenhals, T.; Plaschke, A.; Eisel, D.; Dany, S. C.; Fesser, S.; Erbar, S.; Bates, F.; Schneider, D.; Jesionek, B.; Sanger, B.; Wallisch, A. K.; Feuchter, Y.; Junginger, H.; Krumm, S. A.; Heinen, A. P.; Adams-Quack, P.; Schlereth, J.; Schille, S.; Kroner, C.; de la Caridad Guimil Garcia, R.; Hiller, T.; Fischer, L.; Sellers, R. S.; Choudhary, S.; Gonzalez, O.; Vascotto, F.; Gutman, M. R.; Fontenot, J. A.; Hall-Ursone, S.; Brasky, K.; Griffor, M. C.; Han, S.; Su, A. A. H.; Lees, J. A.; Nedoma, N. L.; Mashalidis, E. H.; Sahasrabudhe, P. V.; Tan, C. Y.; Pavliakova, D.; Singh, G.; Fontes-Garfias, C.; Pride, M.; Scully, I. L.; Ciolino, T.; Obregon, J.; Gazi, M.; Carrion, R., Jr.; Alfson, K. J.; Kalina, W. V.; Kaushal, D.; Shi, P. Y.; Klamp, T.; Rosenbaum, C.; Kuhn, A. N.; Tureci, O.; Dormitzer, P. R.; Jansen, K. U.; Sahin, U. BNT162b vaccines protect rhesus macaques from SARS-CoV-2. *Nature* **2021**, *592*, 283−289.
(13) Hou, Y. J.; Okuda, K.; Edwards, C. E.; Martinez, D. R.; Asakura, T.; Dinnon, K. H., 3rd; Kato, T.; Lee, R. E.; Yount, B. L.; Mascenik, T. M.; Chen, G.; Olivier, K. N.; Ghio, A.; Tse, L. V.; Leist, S. R.; Gralinski, L. E.; Schafer, A.; Dang, H.; Gilmore, R.; Nakano, S.; Sun, L.; Fulcher, M. L.; Livraghi-Butrico, A.; Nicely, N. I.; Cameron, M.; Cameron, C.; Kelvin, D. J.; de Silva, A.; Margolis, D. M.; Markmann, A.; Bartelt, L.; Zumwalt, R.; Martinez, F. J.; Salvatore, S. P.; Borczuk, A.; Tata, P. R.; Sontake, V.; Kimple, A.; Jaspers, I.; O'Neal, W. K.; Randell, S. H.; Boucher, R. C.; Baric, R. S. SARS-CoV-2 Reverse Genetics Reveals a Variable Infection Gradient in the Respiratory Tract. *Cell* **2020**, *182*, 429−446 e14.
(14) van Doremalen, N.; Purushotham, J. N.; Schulz, J. E.; Holbrook, M. G.; Bushmaker, T.; Carmody, A.; Port, J. R.; Yinda, C. K.; Okumura, A.; Saturday, G.; Amanat, F.; Krammer, F.; Hanley, P. W.; Smith, B. J.; Lovaglio, J.; Anzick, S. L.; Barbian, K.; Martens, C.; Gilbert, S. C.; Lambe, T.; Munster, V. J. Intranasal ChAdOx1 nCoV-19/AZD1222 vaccination reduces viral shedding after SARS-CoV-2 D614G challenge in preclinical models. *Sci. Transl. Med.* **2021**, *13*, eabh0755.
(15) Cao, H.; Mai, J.; Zhou, Z.; Li, Z.; Duan, R.; Watt, J.; Chen, Z.; Bandara, R. A.; Li, M.; Ahn, S. K.; Poon, B.; Christie-Holmes, N.; Gray-Owen, S. D.; Banerjee, A.; Mossman, K.; Kozak, R.; Mubareka, S.; Rini, J. M.; Hu, J.; Liu, J. Intranasal HD-Ad vaccine protects the upper and lower respiratory tracts of hACE2 mice against SARS-CoV-2. *Cell Biosci.* **2021**, *11*, 202.
(16) Zhou, R.; Wang, P.; Wong, Y. C.; Xu, H.; Lau, S. Y.; Liu, L.; Mok, B. W.; Peng, Q.; Liu, N.; Woo, K. F.; Deng, S.; Tam, R. C.; Huang, H.; Zhang, A. J.; Zhou, D.; Zhou, B.; Chan, C. Y.; Du, Z.; Yang, D.; Au, K. K.; Yuen, K. Y.; Chen, H.; Chen, Z. Nasal prevention of SARS-CoV-2 infection by intranasal influenza-based boost vaccination in mouse models. *EBioMedicine* **2022**, *75*, 103762.
(17) Hassan, A. O.; Shrihari, S.; Gorman, M. J.; Ying, B.; Yaun, D.; Raju, S.; Chen, R. E.; Dmitriev, I. P.; Kashentseva, E.; Adams, L. J.; Mann, C.; Davis-Gardner, M. E.; Suthar, M. S.; Shi, P. Y.; Saphire, E. O.; Fremont, D. H.; Curiel, D. T.; Alter, G.; Diamond, M. S. An intranasal vaccine durably protects against SARS-CoV-2 variants in mice. *Cell Rep.* **2021**, *36*, 109452.
(18) Kiyono, H.; Fukuyama, S. NALT- versus Peyer's-patch-mediated mucosal immunity. *Nat. Rev. Immunol.* **2004**, *4*, 699−710.
(19) Yang, F.; Meng, L.; Lin, S.; Wu, F.; Liu, J. Polyethyleneimine-complexed charge-reversed yeast cell walls for the enhanced oral delivery of pseudovirus-based antigens. *Chem. Commun.* **2021**, *57*, 12768−12771.
(20) Yuan, R.; Li, Y.; Han, S.; Chen, X.; Chen, J.; He, J.; Gao, H.; Yang, Y.; Yang, S.; Yang, Y. Fe-Curcumin Nanozyme-Mediated Reactive Oxygen Species Scavenging and Anti-Inflammation for Acute Lung Injury. *ACS Cent. Sci.* **2022**, *8*, 10−21.
(21) Sung, H. D.; Kim, N.; Lee, Y.; Lee, E. J. Protein-Based Nanoparticle Vaccines for SARS-CoV-2. *Int. J. Mol. Sci.* **2021**, *22*, 13445.
(22) Cho, K. J.; Shin, H. J.; Lee, J. H.; Kim, K. J.; Park, S. S.; Lee, Y.; Lee, C.; Park, S. S.; Kim, K. H. The crystal structure of ferritin from Helicobacter pylori reveals unusual conformational changes for iron uptake. *J. Mol. Biol.* **2009**, *390*, 83−98.
(23) Kanekiyo, M.; Wei, C. J.; Yassine, H. M.; McTamney, P. M.; Boyington, J. C.; Whittle, J. R.; Rao, S. S.; Kong, W. P.; Wang, L.; Nabel, G. J. Self-assembling influenza nanoparticle vaccines elicit broadly neutralizing H1N1 antibodies. *Nature* **2013**, *499*, 102−106.
(24) Kanekiyo, M.; Bu, W.; Joyce, M. G.; Meng, G.; Whittle, J. R.; Baxa, U.; Yamamoto, T.; Narpala, S.; Todd, J. P.; Rao, S. S.; McDermott, A. B.; Koup, R. A.; Rossmann, M. G.; Mascola, J. R.; Graham, B. S.; Cohen, J. I.; Nabel, G. J. Rational Design of an Epstein-Barr Virus Vaccine Targeting the Receptor-Binding Site. *Cell* **2015**, *162*, 1090−1100.
(25) Wuertz, K. M.; Barkei, E. K.; Chen, W. H.; Martinez, E. J.; Lakhal-Naouar, I.; Jagodzinski, L. L.; Paquin-Proulx, D.; Gromowski, G. D.; Swafford, I.; Ganesh, A.; Dong, M.; Zeng, X.; Thomas, P. V.; Sankhala, R. S.; Hajduczki, A.; Peterson, C. E.; Kuklis, C.; Soman, S.; Wieczorek, L.; Zemil, M.; Anderson, A.; Darden, J.; Hernandez, H.; Grove, H.; Dussupt, V.; Hack, H.; de la Barrera, R.; Zarling, S.; Wood, J. F.; Froude, J. W.; Gagne, M.; Henry, A. R.; Mokhtari, E. B.; Mudvari, P.; Krebs, S. J.; Pekosz, A. S.; Currier, J. R.; Kar, S.; Porto, M.; Winn, A.; Radzyminski, K.; Lewis, M. G.; Vasan, S.; Suthar, M.; Polonis, V. R.; Matyas, G. R.; Boritz, E. A.; Douek, D. C.; Seder, R. A.; Daye, S. P.; Rao, M.; Peel, S. A.; Joyce, M. G.; Bolton, D. L.; Michael, N. L.; Modjarrad, K. A SARS-CoV-2 spike ferritin nanoparticle vaccine protects hamsters against Alpha and Beta virus variant challenge. *npj Vaccines* **2021**, *6*, 129.
(26) Gu, M.; Torres, J. L.; Li, Y.; Van Ry, A.; Greenhouse, J.; Wallace, S.; Chiang, C. I.; Pessaint, L.; Jackson, A. M.; Porto, M.; Kar, S.; Li, Y.; Ward, A. B.; Wang, Y. One dose of COVID-19 nanoparticle vaccine REVC-128 protects against SARS-CoV-2 challenge at two weeks post-immunization. *Emerging Microbes Infect.* **2021**, *10*, 2016−2029.
(27) Powell, A. E.; Zhang, K.; Sanyal, M.; Tang, S.; Weidenbacher, P. A.; Li, S.; Pham, T. D.; Pak, J. E.; Chiu, W.; Kim, P. S. A Single Immunization with Spike-Functionalized Ferritin Vaccines Elicits Neutralizing Antibody Responses against SARS-CoV-2 in Mice. *ACS Cent. Sci.* **2021**, *7*, 183−199.
(28) Huleatt, J. W.; Nakaar, V.; Desai, P.; Huang, Y.; Hewitt, D.; Jacobs, A.; Tang, J.; McDonald, W.; Song, L.; Evans, R. K.; Umlauf, S.; Tussey, L.; Powell, T. J. Potent immunogenicity and efficacy of a universal influenza vaccine candidate comprising a recombinant fusion protein linking influenza M2e to the TLR5 ligand flagellin. *Vaccine* **2008**, *26*, 201−214.
(29) McDonald, W. F.; Huleatt, J. W.; Foellmer, H. G.; Hewitt, D.; Tang, J.; Desai, P.; Price, A.; Jacobs, A.; Takahashi, V. N.; Huang, Y.; Nakaar, V.; Alexopoulou, L.; Fikrig, E.; Powell, T. J. A West Nile virus recombinant protein vaccine that coactivates innate and adaptive immunity. *J. Infect. Dis.* **2007**, *195*, 1607−1617.
(30) Song, L.; Nakaar, V.; Kavita, U.; Price, A.; Huleatt, J.; Tang, J.; Jacobs, A.; Liu, G.; Huang, Y.; Desai, P.; Maksymiuk, G.; Takahashi, V.; Umlauf, S.; Reiserova, L.; Bell, R.; Li, H.; Zhang, Y.; McDonald, W. F.; Powell, T. J.; Tussey, L. Efficacious recombinant influenza vaccines produced by high yield bacterial expression: a solution to global pandemic and seasonal needs. *PLoS One* **2008**, *3*, No. e2257.
(31) Burdelya, L. G.; Krivokrysenko, V. I.; Tallant, T. C.; Strom, E.; Gleiberman, A. S.; Gupta, D.; Kurnasov, O. V.; Fort, F. L.; Osterman, A. L.; Didonato, J. A.; Feinstein, E.; Gudkov, A. V. An agonist of toll-like receptor 5 has radioprotective activity in mouse and primate models. *Science* **2008**, *320*, 226−230.
(32) Saunders, K. O.; Lee, E.; Parks, R.; Martinez, D. R.; Li, D.; Chen, H.; Edwards, R. J.; Gobeil, S.; Barr, M.; Mansouri, K.; Alam, S. M.; Sutherland, L. L.; Cai, F.; Sanzone, A. M.; Berry, M.; Manne, K.; Bock, K. W.; Minai, M.; Nagata, B. M.; Kapingidza, A. B.; Azoitei, M.; Tse, L. V.; Scobey, T. D.; Spreng, R. L.; Rountree, R. W.; DeMarco, C. T.; Denny, T. N.; Woods, C. W.; Petzold, E. W.; Tang, J.; Oguin, T. H., 3rd; Sempowski, G. D.; Gagne, M.; Douek, D. C.; Tomai, M. A.; Fox, C. B.; Seder, R.; Wiehe, K.; Weissman, D.; Pardi, N.; Golding, H.; Khurana, S.; Acharya, P.; Andersen, H.; Lewis, M. G.; Moore, I. N.; Montefiori, D. C.; Baric, R. S.; Haynes, B. F. Neutralizing antibody vaccine for

https://doi.org/10.1021/acsabm.2c00328
ACS Appl. Bio Mater. XXXX, XXX, XXX−XXX

pandemic and pre-emergent coronaviruses. *Nature* **2021**, *594*, 553−559.
(33) Tang, S.; Xuan, B.; Ye, X.; Huang, Z.; Qian, Z. A Modular Vaccine Development Platform Based on Sortase-Mediated Site-Specific Tagging of Antigens onto Virus-Like Particles. *Sci. Rep.* **2016**, *6*, 25741.
(34) Kang, Y. F.; Sun, C.; Zhuang, Z.; Yuan, R. Y.; Zheng, Q.; Li, J. P.; Zhou, P. P.; Chen, X. C.; Liu, Z.; Zhang, X.; Yu, X. H.; Kong, X. W.; Zhu, Q. Y.; Zhong, Q.; Xu, M.; Zhong, N. S.; Zeng, Y. X.; Feng, G. K.; Ke, C.; Zhao, J. C.; Zeng, M. S. Rapid Development of SARS-CoV-2 Spike Protein Receptor-Binding Domain Self-Assembled Nanoparticle Vaccine Candidates. *ACS Nano* **2021**, *15*, 2738−2752.
(35) Zhang, B.; Chao, C. W.; Tsybovsky, Y.; Abiona, O. M.; Hutchinson, G. B.; Moliva, J. I.; Olia, A. S.; Pegu, A.; Phung, E.; Stewart-Jones, G. B. E.; Verardi, R.; Wang, L.; Wang, S.; Werner, A.; Yang, E. S.; Yap, C.; Zhou, T.; Mascola, J. R.; Sullivan, N. J.; Graham, B. S.; Corbett, K. S.; Kwong, P. D. A platform incorporating trimeric antigens into self-assembling nanoparticles reveals SARS-CoV-2-spike nanoparticles to elicit substantially higher neutralizing responses than spike alone. *Sci. Rep.* **2020**, *10*, 18149.
(36) Rahikainen, R.; Rijal, P.; Tan, T. K.; Wu, H. J.; Andersson, A. C.; Barrett, J. R.; Bowden, T. A.; Draper, S. J.; Townsend, A. R.; Howarth, M. Overcoming Symmetry Mismatch in Vaccine Nanoassembly through Spontaneous Amidation. *Angew Chem., Int. Ed.* **2021**, *60*, 321−330.
(37) Tang, S.; Liu, Z.; Xu, W.; Li, Q.; Han, T.; Pan, D.; Yue, N.; Wu, M.; Liu, Q.; Yuan, W.; Huang, Z.; Zhou, D.; Zhou, W.; Qian, Z. Versatile Functionalization of Ferritin Nanoparticles by Intein-Mediated Trans-Splicing for Antigen/Adjuvant Co-delivery. *Nano Lett.* **2019**, *19*, 5469−5475.
(38) Tang, S.; Han, T.; Wang, Z.; Yue, N.; Liu, Z.; Tang, S.; Yang, X.; Zhang, Z.; Zhou, Y.; Yuan, W.; Hao, H.; Sleman, S.; Pan, D.; Xuan, B.; Zhou, W.; Qian, Z. Facile and Modular Pipeline for Protein-Specific Antibody Customization. *ACS Appl. Bio Mater.* **2020**, *3*, 4380−4387.
(39) Wang, Z.; Tang, S.; Yue, N.; Qian, Z.; Zhou, S. Development of HBc virus-like particles as modular nanocarrier by intein-mediated trans-splicing. *Biochem. Biophys. Res. Commun.* **2021**, *534*, 891−895.
(40) Wang, L.; Wang, X.; Yang, F.; Liu, Y.; Meng, L.; Pang, Y.; Zhang, M.; Chen, F.; Pan, C.; Lin, S.; Zhu, X.; Leong, K. W.; Liu, J. Systemic antiviral immunization by virus-mimicking nanoparticles-decorated erythrocytes. *Nano Today* **2021**, *40*, 101280.
(41) Kim, S.; Kim, G. S.; Seo, J.; Gowri Rangaswamy, G.; So, I. S.; Park, R. W.; Lee, B. H.; Kim, I. S. Double-Chambered Ferritin Platform: Dual-Function Payloads of Cytotoxic Peptides and Fluorescent Protein. *Biomacromolecules* **2016**, *17*, 12−19.
(42) He, D.; Marles-Wright, J. Ferritin family proteins and their use in bionanotechnology. *New Biotechnol.* **2015**, *32*, 651−657.
(43) Li, M.; Wang, Y.; Sun, Y.; Cui, H.; Zhu, S. J.; Qiu, H. J. Mucosal vaccines: Strategies and challenges. *Immunol. Lett.* **2020**, *217*, 116−125.
(44) Nacer, A.; Carapau, D.; Mitchell, R.; Meltzer, A.; Shaw, A.; Frevert, U.; Nardin, E. H. Imaging murine NALT following intranasal immunization with flagellin-modified circumsporozoite protein malaria vaccines. *Mucosal Immunol.* **2014**, *7*, 304−314.
(45) Wu, S.; Huang, J.; Zhang, Z.; Wu, J.; Zhang, J.; Hu, H.; Zhu, T.; Zhang, J.; Luo, L.; Fan, P.; Wang, B.; Chen, C.; Chen, Y.; Song, X.; Wang, Y.; Si, W.; Sun, T.; Wang, X.; Hou, L.; Chen, W. Safety, tolerability, and immunogenicity of an aerosolised adenovirus type-5 vector-based COVID-19 vaccine (Ad5-nCoV) in adults: preliminary report of an open-label and randomised phase 1 clinical trial. *Lancet Infect. Dis.* **2021**, *21*, 1654−1664.
(46) Lapuente, D.; Fuchs, J.; Willar, J.; Vieira Antao, A.; Eberlein, V.; Uhlig, N.; Issmail, L.; Schmidt, A.; Oltmanns, F.; Peter, A. S.; Mueller-Schmucker, S.; Irrgang, P.; Fraedrich, K.; Cara, A.; Hoffmann, M.; Pohlmann, S.; Ensser, A.; Pertl, C.; Willert, T.; Thirion, C.; Grunwald, T.; Uberla, K.; Tenbusch, M. Protective mucosal immunity against SARS-CoV-2 after heterologous systemic prime-mucosal boost immunization. *Nat. Commun.* **2021**, *12*, 6871.
(47) Poland, G. A.; Ovsyannikova, I. G.; Kennedy, R. B. SARS-CoV-2 immunity: review and applications to phase 3 vaccine candidates. *Lancet* **2020**, *396*, 1595−1606.
(48) Chung, N. H.; Chen, Y. C.; Yang, S. J.; Lin, Y. C.; Dou, H. Y.; Hui-Ching Wang, L.; Liao, C. L.; Chow, Y. H. Induction of Th1 and Th2 in the protection against SARS-CoV-2 through mucosal delivery of an adenovirus vaccine expressing an engineered spike protein. *Vaccine* **2022**, *40*, 574−586.

https://doi.org/10.1021/acsabm.2c00328
ACS Appl. Bio Mater. XXXX, XXX, XXX−XXX